

STRENGTH VARIATIONS WITH DEFORMATION IN UNCONSOLIDATED ROCK AFTER WATER BREAKTHROUGH

Gang Han, Maurice B. Dusseault, University of Waterloo

ABSTRACT

Reservoir rock may be weakened significantly after water breakthrough because of capillary strength changes with water saturation, and by the effects of chemical reactions between formation water and rock cementation. Because of weakening, the rock will behave differently in single phase (oil) and in water-oil fluid environments. Two analytical models are developed to study the changes in rock capillary strength with water saturation and deformation in two different loading states: confined and detached (unconfined).

Based on the model calculations, it is found that capillary strength increases rapidly to a peak value with water saturation at a low saturation state, and then decreases gradually to become zero if the sand becomes 100% water saturated. The greater the distance between particles in a detached state, the higher the water saturation needed to maximize capillary strength. Furthermore, the peak capillary strength is affected by several factors, including interparticle distance, liquid contact angle, particle size, and interphasic surface tension. The more the particles are detached or squeezed, the lower the peak strength. Small particle size, large interphase surface tension, and low contact angle result in high capillary strength.

By introducing the concept of solid strain from rock mechanics into capillary models, it can be shown that, at the same amount of water in the liquid bridge, capillary strength keeps decreasing with rock compression. Conversely, it increases slightly with extensional deformation before reaching a peak, and then continuously decreasing as extensional deformation continues. The rate of decrease of rock strength with compressional deformation is much faster than in the case of extensional deformation.

The models and results can be used to quantify the failure risk associated with loading a reservoir rock after water breakthrough, allowing more quantitative well management procedures.

INTRODUCTION

Rock instability resulting from water breakthrough is a common problem for oil industry. It is estimated that, on average, oil companies today produce three barrels of water for each barrel of oil [1], seventy percent of which comes from unconsolidated rock. Many experiments have been conducted to study the strength variations associated with water content changes in unconsolidated sand [2,3,4,5,6,7] and chalk [8,9]. All researchers

found that rock strength in a fully water-saturated state is decreased to some extent (from 7% [4] to 50% [7]), compared to the dry state.

Studying the relationship between rock strength and water saturation in the laboratory tends to be a challenge for physicists. It is generally believed that rock strength decreases with water saturation [9,10], while some results suggested a small increase in water saturation (up to 3%) is found to provide enough cohesive strength to stabilize a sand arch around an opening, and massive sand production does not occur until water saturation is above 32% [10]. Though most studies agree that capillarity is an important factor contributing to rock stability under two-phase flow in unconsolidated reservoirs, there is a lack of quantitative description of the capillary strength behavior in multiphase systems. Han and Dusseault [11] provided a method to quantify capillary force, showing that it may be higher than the fluid seepage force that acts as the major local destabilizing force in sand mobilization. However, the simplifications in this model, such as a tangential particle contact assumption, limit the applications since most particles are either detached or squeezed (compressed), and will undergo further deformations as loads change.

In this paper, two analytical models are proposed to quantitatively describe capillary strength variations with water saturation for different contact fabrics, and to predict strength behavior in particular loading states at specific water saturations.

MODEL DEVELOPMENT

Besides tangential contacts, there are several other contact fabrics that may exist between particles in a granular geological medium: these have been classified, for example, as floating contacts, sutured contacts, convex-concave contacts, and long contacts [12]. Figure 1 summarizes this classification into two possible microscopic cases: uniform particles are detached from each other (which may simply be an artifact of the sampling and preparation procedure); or squeezed and overlapped to form convex-concave or long contacts. These two cases are analyzed in detail.

Detached Model ($a > 0$)

By assuming that the shape of the liquid bridge is a toroid characterized by a radius of curvature r (Figure 1), the widely accepted formula to calculate capillary pressure can be derived:

$$\Delta P = \gamma \left(\frac{1}{r_1} - \frac{1}{r} \right) \quad (1)$$

The precision of the toroid approximation is within 10% of the value obtained by numerical solution of the Laplace-Young equation [13]. The ‘‘Pressure Difference Method’’ is used to calculate capillary force resulting from capillary pressure since it is demonstrated to be more reasonable [11]:

$$F_c = \pi (R \sin \alpha)^2 \Delta P \quad (2)$$

Based on some assumptions [14,15], rock tensile strength can be related to capillary force F_c of a single bond by [14]

$$\sigma_T = \frac{1-\phi}{\phi} \frac{F_c}{4R^2} \quad (3)$$

Therefore, based on a linear Mohr-Coulomb yield criterion, the UCS (Unconfined Compressive Strength) can be approximately expressed as

$$\sigma_{UCS} = \frac{1-\phi}{\phi} \frac{\sin \phi}{1-\sin \phi} \frac{F_c}{2R^2} \quad (4)$$

which illustrates that, for unconsolidated sand, rock strength is related to rock porosity, friction angle, capillary force, and particle size.

If water in the unit cell (shaded area in Figure 2) is only present in the liquid bridge (i.e. low water saturation), water saturation can be expressed as

$$S_w = \frac{4[x_p y_p - (A_1 + A_2)]}{V\phi} \quad (5)$$

where the porosity ϕ of the unit is

$$\phi = 1 - \frac{\pi R^2}{2R \cdot (2R + 2a)} = 1 - \frac{\pi}{4(1+k)} \quad (6)$$

where k is the ratio of half distance between particles to particle radius, i.e. $k = a/R$. The coordinates of point P in Figure 1 are

$$x_p = R \sin \alpha; \quad y_p = R + a - R \cos \alpha \quad (7)$$

while A_1 and A_2 in Eq. (5) can be geometrically expressed as

$$A_1 = \frac{\alpha}{2} R^2 - \frac{1}{2} (R + a - y_p) x_p \quad (8)$$

$$A_2 = \left(\frac{\pi}{4} - \frac{\alpha + \theta}{2} \right) r^2 - \frac{1}{2} y_p r \sin(\alpha + \theta) \quad (9)$$

When the contact angle $\theta \neq 0$, the radius r can be determined by

$$r = \frac{R + a - R \cos \alpha}{\cos(\alpha + \theta)} = \frac{1+k - \cos \alpha}{\cos(\alpha + \theta)} \cdot R \quad (10)$$

Consequently the expression of water saturation becomes

$$(1+k) \left[1 - \frac{\pi}{4(1+k)} \right] S_w = -\frac{\alpha}{2} + (1+k) \sin \alpha - \frac{1}{4} \sin 2\alpha - \left[\frac{\pi}{4} - \frac{\alpha + \theta}{2} - \frac{1}{4} \sin 2(\alpha + \theta) \right] \left[\frac{1+k - \cos \alpha}{\cos(\alpha + \theta)} \right]^2 \quad (11)$$

When the contact angle $\theta = 0$, this equation can be simplified:

$$(1+k) \left[1 - \frac{\pi}{4(1+k)} \right] S_w = -\frac{\pi}{4} + (1+k) \sin \alpha - \left(\frac{\pi}{4} - \frac{\alpha}{2} - \frac{1}{4} \sin 2\alpha \right) \left[\left(\frac{1+k}{\cos \alpha} \right)^2 - \frac{2(1+k)}{\cos \alpha} \right] \quad (12)$$

As a conclusion, an expression of capillary force (Eq.2) can be achieved as a function of water saturation, the distance between particles, and particle radius.

Squeezed Model ($a < 0$)

For the case of squeezed particles (i.e. $a < 0$, Figure 1), the angle β is introduced to describe the squeezed extent, and it can be determined by

$$\beta = \arccos(1 - k) \quad (13)$$

Following the steps described for the detached model, other parameters used to determine capillary force become

$$x_p = R \sin \alpha; \quad y_p = R - a - R \cos \alpha \quad (14)$$

$$r = \frac{R - a - R \cos \alpha}{\cos(\alpha + \theta)} = \frac{1 - k - \cos \alpha}{\cos(\alpha + \theta)} \cdot R \quad (15)$$

$$A_1 = \left(\frac{\alpha - \beta}{2}\right)R^2 - \frac{1}{4}R^2(\sin 2\alpha - \sin 2\beta) \quad (16)$$

$$A_2 = \left(\frac{\pi}{4} - \frac{\alpha + \theta}{2}\right)r^2 - \frac{1}{4}r^2 \sin(2(\alpha + \theta)) \quad (17)$$

$$\phi = 1 - \frac{\pi R^2 - R^2(2\beta - \sin 2\beta)}{2R \cdot (2R - 2a)} = 1 - \frac{\pi - 2\beta + \sin 2\beta}{4(1 - k)} \quad (18)$$

Therefore, water saturation can be expressed as

$$(1 - k) \left[1 - \frac{\pi - 2\beta + \sin 2\beta}{4(1 - k)} \right] S_w = \frac{-\alpha + \beta}{2} + (1 - k) \sin \alpha - \frac{1}{4}(\sin 2\alpha + \sin 2\beta) - \left[\frac{\pi}{4} - \frac{\alpha + \theta}{2} - \frac{1}{4} \sin 2(\alpha + \theta) \right] \left[\frac{1 - k - \cos \alpha}{\cos(\alpha + \theta)} \right]^2 \quad (19)$$

Thus, for each water saturation the volume angle α can be determined, as well as the other parameters needed for calculating capillary force and capillary strength.

Introduction of Strain

One character of capillary force is that it does not break abruptly with rock deformation, as does mineral cohesion, which is sensitive to strain (usually, an extensional strain of less than 0.2% is sufficient to rupture cementitious bonds). This means that before the sands deform to the extent that the grains are fully disaggregated, the capillary force still exists during the progressive weakening, dilation and separation processes. For brittle mineral cohesion destroyed by shear distortion, capillary cohesion remains unaffected.

In Figure 1 the volumetric deformation of the particles can be expressed as

$$\varepsilon = \frac{\Delta V}{V} = \frac{2R(2R + 2a) - 2R \cdot 2R}{2R \cdot 2R} = \frac{a}{R} \quad (20)$$

Coincidentally, it is equal to k , the ratio of the half distance between particles to the particle radius. Therefore the models developed to calculate capillary strength for detached and squeezed particles can be used to describe the variations of capillary strength with rock

deformation, except that, instead of the water saturation, water volume in the liquid bridge between particles should remain constant. The water volume in the liquid bridge (Q_w) for the detached particle state can be calculated by

$$Q_w = 4R^2 \left(1 + k - \frac{\pi}{4}\right) \cdot S_w \quad (21)$$

whereas for the compressed case it is:

$$Q_w = 4R^2 \left[(1-k) \left(1 - \frac{1}{2} \sin \beta\right) - \frac{\pi}{4} + \frac{1}{2} \beta \right] \cdot S_w \quad (22)$$

CALCULATIONS AND DISCUSSION

Compared to the tangential grain contact model developed elsewhere [11], the models presented here can be used to analytically describe the variations of capillary strength with water saturation and the behavior of capillary strength at a specific water saturation but with different strain. It should be noted that there are some assumptions made during the model development, such as:

- particles consist of uniform spheres distributed statistically uniformly;
- the variable bond strength between particles can be replaced by a mean value that is applicable throughout the whole rock;
- water is distributed evenly inside the rock; and,
- liquid bridge formed between particles can be described as a toroid.

Whereas these may be viewed as limitations to the applicability of the model, we believe that because the model captures the essential physics, adjustments and calibration can easily be incorporated so as to give useful results in practice.

Capillary Strength vs. Water Saturation

The parameters used in the models are listed in Table 1 (unless otherwise specified). This parameter list clearly shows the simplicity of the models: only particle radius, surface tension, contact angle, porosity, and friction angle are needed to estimate the magnitude of capillary strength.

Experiments [10] show that a stable arch starts to develop even with a small increase in water saturation ($S_w > 3\%$) in a two-phase environment, whereas such an arch cannot be stable in a monophasic condition. Furthermore, the sand starts to flow into the wellbore when $S_w > 20\%$, and massive sand production occurs if $S_w > 32\%$. Figure 3 and Figure 4 demonstrate the calculated relations between capillary strength and water saturation for the detached and compressed states, respectively. Compared to tangentially contacting particles (dashed lines in the figures), where the strength continuously decreases with water saturation, when particles are separated or compressed (solid lines), capillary strength will not reach its peak until some critical water saturation. Furthermore, the greater the distance between particles, either positive (detached) or negative (squeezed), the higher the water saturation that is needed to attain the maximum capillary strength. This is reasonable because there will be more water needed for widely spaced particles to form a strong liquid bridge than for more closely spaced particles.

Factors Affecting the Capillary Strength

In order to clarify the factors affecting the peak capillary strength, sensitivity analyses with respect to several parameters were carried out. Water saturation is of course fundamentally important in all these cases.

Capillary peak strength is strongly affected by the distance between particles. For detached particles, the larger the distance (which is characterized by larger k values in Figure 3), the lower the value of peak strength. For the compressed condition (Figure 4), the more the particles are squeezed, the lower the capillary strength is. Also, when the magnitudes of separation and compression are the same (e.g. $k = 0.01$ and $k = -0.01$), the capillary strength in the array of separated particles ($k = 0.01$) is much higher than the capillary strength in the squeezed arrays ($k = -0.01$).

At the same water saturation, the capillary strength increases if the contact angle decreases. Figure 5 shows the relation between capillary strength and contact angle when $k = 0.01$. The peak strength increases from 200 Pa to about 900 Pa when contact angle changed from one radian (57.3°) to zero.

A smaller particle size results in a higher capillary strength (Figure 6). Since the particle size of most reservoir rocks ranges from 0.025mm to 0.25mm, the strength formed by capillary force may reach the magnitude of several kPa.

In addition, capillary strength is linearly related to the magnitude of the surface tension between the fluids [11].

Capillary Strength Behaviour during Deformation

Figure 7 illustrates the calculations listed in Table 2. Following the conventions of rock mechanics, a negative sign for deformation means extension, whereas a positive sign means compression. Interestingly, when water volume in the liquid bridge is constant, the tensile strength resulting from capillary forces keeps decreasing with rock compression, whereas it increases slightly with extensional deformation before beginning to continuously decrease as extensional strain increases. This difference becomes more obvious when there is more water in the bridge, as demonstrated by the curve of $Q_w = 6.87 \times 10^{-9} \text{ m}^3$ in Figure 7. Because of the difficulty of executing laboratory experiments under the challenging conditions of no external confining stress in a granular medium, in the petroleum industry there is as yet no experimental data available to verify the character of this relationship. However there are some experiments reported in the chemical engineering literature rather than small mineral particles, and these data show the same effect of detached distance. For example, the spheres Mason and Clark (Figure 8) used were oil-wet, fully immersed in water, and with a radius of 15 mm. Each curve corresponds to a constant water volume in the liquid bridge, and it generally decreases with the separated distance shortly after a slight increase (same as the curves with negative k in Figure 7).

The decrease rate of the sand capillary strength under compression is much faster than that of the sand under extension. For example, when the water bridge volume is $1.72 \times 10^{-9} \text{ m}^3$, and the volumetric strain is 0.02, the tensile strength will decrease from 383 Pa to 95 Pa in compression, and from 383 Pa to 316 Pa in extension (Table 2). In reservoir situations, the intact reservoir sand inevitably has to experience compression due to the increases in effective stress during reservoir depletion, and in these conditions, the capillary strength may decrease rapidly with water saturation. On the other hand, if rock has experienced considerable compaction beforehand and particles are at large originally in a squeezed state when oil production starts, the capillary strength can be expected to be relatively small, depending on the degree of compaction.

CONCLUSIONS

Two analytical models are developed to quantify the variations of capillary strength for different contact fabrics of spherical mineral particles. Based on model calculations, some conclusions can be suggested:

- When particles are detached or in compressional contact, capillary strength will firstly increase to some peak value before continuously decreasing with water saturation. The farther the distance between particles, either positive (detached) or negative (squeezed), the higher the water saturation needed to maximize capillary strength.
- The maximum value of capillary strength is strongly affected by the distance between particles. The more the particles are detached or squeezed, the lower the peak capillary strength that can be achieved.
- At the same water saturation, capillary strength increases if the contact angle decreases.
- Smaller particle size results in higher capillary strengths; for reservoir sand, it is likely to reach the order of several kPa.

Furthermore, by introducing the strain concept that is used in geomechanics, the models can be used to describe the behavior of capillary strength upon loading.

- When the water volume in the liquid bridge between particles is constant, capillary strength keeps decreasing with rock compression whereas it increases slightly with extensional deformation before continuously decreasing. This difference becomes more obvious when there is more water in the bridge.
- The rate of decrease in rock capillary strength with compressional deformation is much faster than for the case of extensional deformation.

Since reservoir rock is usually under compression, capillary strength may decrease rapidly upon further loading.

ACKNOWLEDGMENTS

The authors thank Drs. Denis Heliot, Steve Chan, and John Cook from Schlumberger for having initiated the studies, and for sponsoring the project. The technical

communications with Dr. Bianco, L.C.B. (PetroBras), and advice from the reviewers, Dr. Colin Jones (Weatherford Completion Systems) and Dr. Louis Cuiec (Institut Français du Pétrole), are deeply appreciated.

NOMENCLATURE AND UNITS

a	=	half distance between two particles, m
F_c	=	capillary force, N
k	=	ratio of half distance between particles to particle radius
ΔP	=	capillary pressure, Pa
Q_w	=	water volume in the liquid bridge, m^3
r_l	=	radius of curvature of the liquid bridge in the horizontal plane, m
r	=	radius of curvature of the liquid bridge in the vertical plane, m
R	=	radius of the particles, m
S_w	=	water saturation, fractional (1.0 = 100% water saturation)
UCS	=	uniaxial (unconfined) compressive strength, Pa
x_p, y_p	=	the spatial coordinates of point P(x,y), m
α	=	water volume angle, degree
β	=	angle to describe squeezed extent, degree
ε	=	strain, dimensionless
θ	=	contact angle between fluid and solid, radian
γ	=	surface tension between two fluids, N/m
ϕ	=	porosity of the defined unit, dimensionless
φ	=	friction angle defined in a linear Mohr-Coulomb yield criterion
σ_T	=	tensile strength of rock, Pa

REFERENCES

1. Bailey, B., Crabtree, M., Tyrie, J., Kuchuk, F., Romano, C. and Roodhart, L., "Water Control", *Oil Field Review*, 2000 Spring, 30-50.
2. Bruno, M.S., Bovberg, C.A. and Meyer, R.F., "Some Influences of Saturation and Fluid Flow on Sand Production: Laboratory and Discrete Element Model Investigations", SPE 36534, *the 1996 Annual Technical Conference and Exhibition*, Denver, Colorado, 1996.
3. Dube, A.K. and Singh, B., "Effect of Humidity on Tensile Strength of Sandstone", *J. Mines, Metals and Fuels*, Jan.1972, 20-1, 8-10.
4. Boretti-Onyszkiewicz, W., "Joints in the Flysch Sandstones on the Ground of Strength Examinations", *Proc. 1st Cong. Int. Soc. Rock Mech.*, Lisbon, 1966, 1, 153-157.
5. Tremblay, B., Oldakowski, K. and Settari, A., "Geomechanical Properties of Oil Sands at Low Effective Stress", *the 48th Annual Technical Meeting of the Petroleum Society*, Calgary, Alberta, Canada, Jun. 1997.
6. Colback, P.S.B. and Wiid, B.L., "The Influence of Moisture Content on the Compressive Strength of Rocks", *Proceedings of 3rd Canadian Symposium of Rock Mechanics*, 1965, 65-83.

7. Skjærstein A., Tronvoll, J., Santarelli, F.J. and Jøranson, H., “Effect of Water Breakthrough on Sand Production: Experimental and Field Evidence”, SPE 38806, *SPE Annual Technical Conference and Exhibition*, San Antonio, TX, Oct. 1997.
8. Papamichos, E., Brignoli, M., and Santarelli, F.J., “An Experimental and Theoretical Study of a Partially Saturated Collapsible Rock”, *Mech. of Cohesive-Frictional Materials*, 1997, 2, 251-278.
9. Brignoli, M., Santarelli, F.J., and Righetti, C., “Capillary Phenomena in an Impure Chalk”, *Eurock '94*, Balkema, Rotterdam, 837-843.
10. Bianco, L.C.B., and Halleck, P.M., “Mechanisms of Arch Instability and Sand Production in Two-Phase Saturated Poorly Consolidated Sandstones”, SPE 68932, *the SPE European Formation Damage conference*, Hague, Netherlands, May 2001.
11. Han, G., and Dusseault, M.B., “Quantitative Analysis of Mechanisms for Water-Related Sand Production”, SPE 73737, *the SPE International Symposium and Exhibition on Formation Damage Control held in Lafayette*, LA, U.S.A., Feb. 2002.
12. Taylor, J.M., “Pore Space Reduction in Sandstone”, *Bull. Am. Assoc. Pet. Geol.*, 1950, 34, 701-716.
13. Lian, G., Thornton, C. and Adams, M.J., “Effect of Liquid Bridge Forces on Agglomerate Collisions”, *Powders & Grains*, 1993, 59-64.
14. Schubert, H.: “Tensile Strength of Agglomerates”, *Powder Technology*, 1975, 11, 107-119.
15. Capes, C.E.: “Particle Size Enlargement”, *Handbook of Powder Technology*, 1980, 1, 23-26.
16. Schubert, H., “Capillary Forces – Modelling and Application in Particulate Technology”, *Powder Tech.*, 1984, 47, 105-116.
17. Mason, G., and Clark, W.C., “Liquid Bridges between Spheres”, *Chem. Eng. Sci.*, 1965, 20, 859.

Table 1. Parameters used in the models

R(m)	γ (N/m)	ϕ (%)	ϕ (°)	θ
0.0002	0.036	30	60	0

Table 2. Capillary tensile strength behavior at specific water saturation

k	Water Volume=1.7174E-09 m ³			Water Volume=3.4346E-09m ³			Water Volume=6.8683E-09m ³		
	ΔP	F _c (Dyne)	σ_T	ΔP	F _c (Dyne)	σ_T	ΔP	F _c (Dyne)	σ_T
-0.08	188.7574	0.089554	13.06001	488.591	0.610301	89.00217	250.5626	0.78676	114.7358
-0.05	1191.896	0.869253	126.766	698.2419	1.320736	192.6074	235.773	0.986264	143.8302
-0.02	1416.93	2.169869	316.4392	594.8292	1.827829	266.5584	161.4966	0.895601	130.6084
-0.01	1243.646	2.484285	362.2916	517.0283	1.856671	270.7645	131.3779	0.795269	115.9767
0	1025.181	2.623638	382.6139	434.2228	1.806123	263.3929	101.048	0.664608	96.92201
0.002	935.8183	1.857967	270.9535	401.9196	1.363058	198.7794	89.96591	0.500901	73.04806
0.005	827.2862	1.448839	211.289	360.3461	1.099887	160.4001	75.11642	0.382281	55.74936
0.01	687.1153	1.06158	154.8138	302.7574	0.828924	120.8847	53.50559	0.247369	36.07462
0.02	493.4774	0.653639	95.32238	215.477	0.513431	74.87533	18.36384	0.074687	10.8918
0.05	199.2422	0.205365	29.94904	62.64323	0.117316	17.10852			

Note: negative k means squeezed state while positive k means detached state.

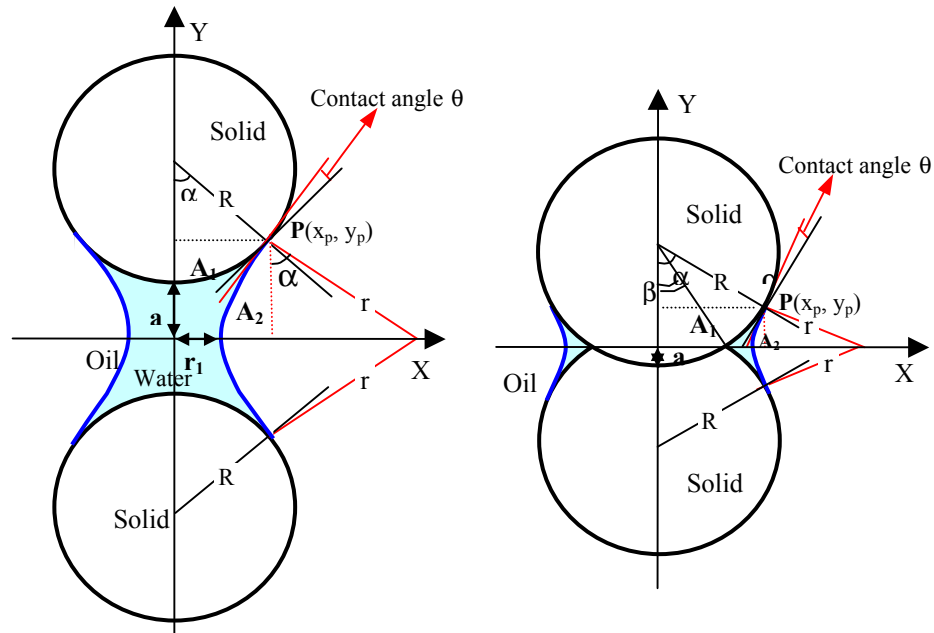


Figure 1. Models for capillary strength (Left: detached state; Right: squeezed state)

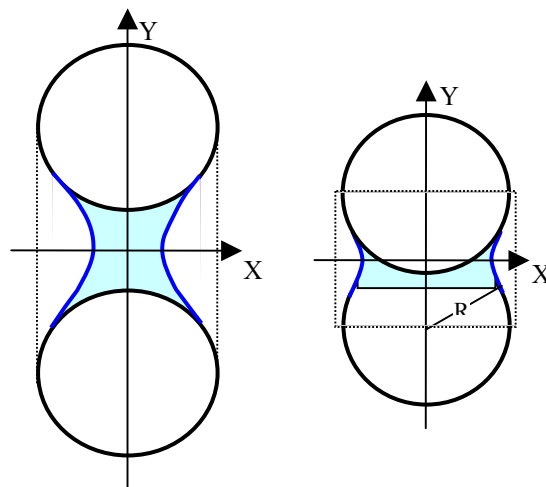


Figure 2. Definition of the unit (Left: detached state; Right: squeezed state)

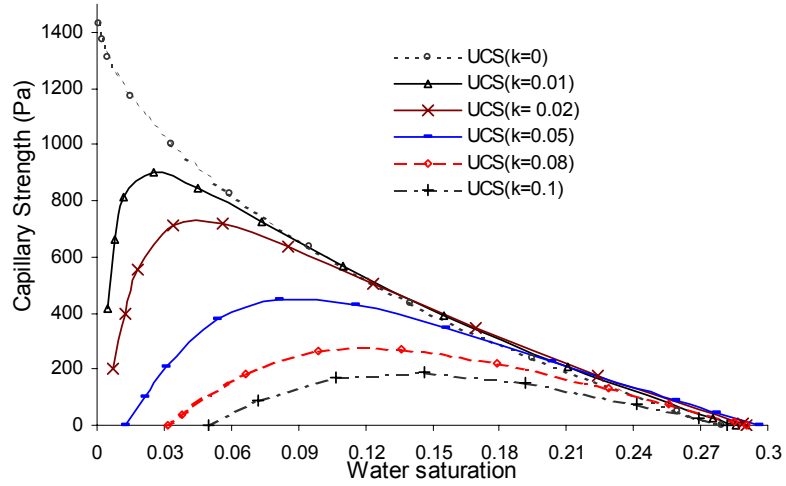


Figure 3. Capillary Strength (UCS) variations with water saturation (detached state)

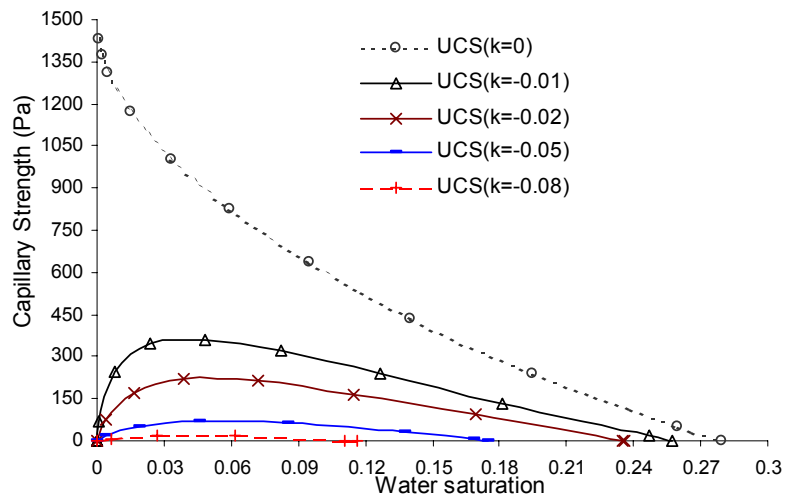


Figure 4. Capillary Strength (UCS) variations with water saturation (squeezed state)

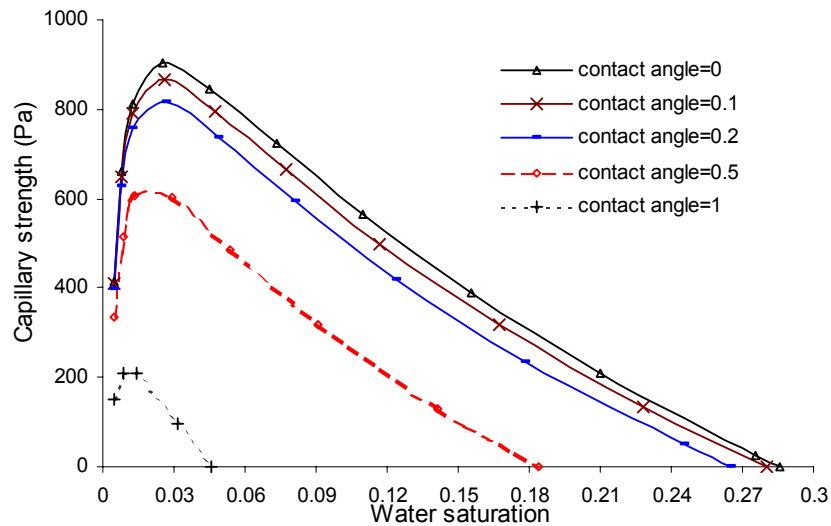


Figure 5. Effect of contact angle on capillary strength (UCS) when $k = a/R = 0.01$

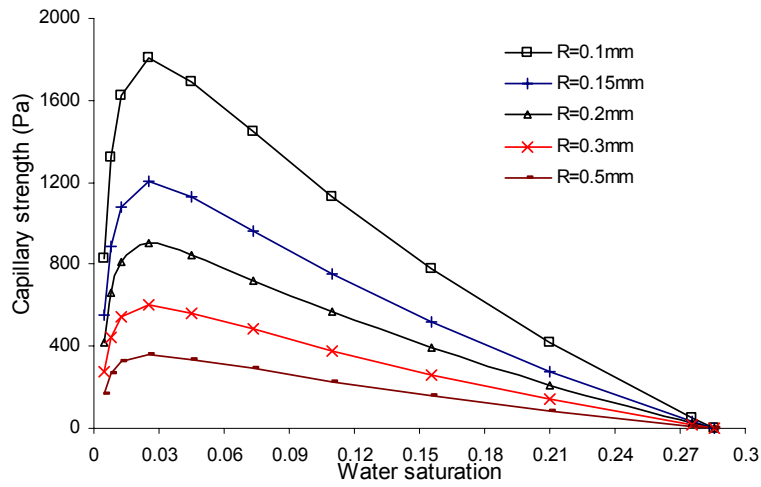


Figure 6. Effect of particle size on capillary strength (UCS) when $k=0.01$

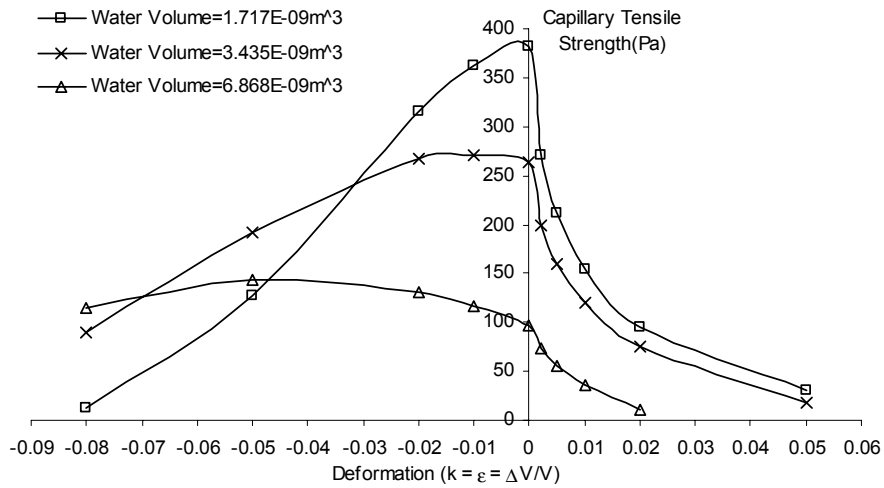


Figure 7. Behaviors of capillary tensile strength at specific water saturation

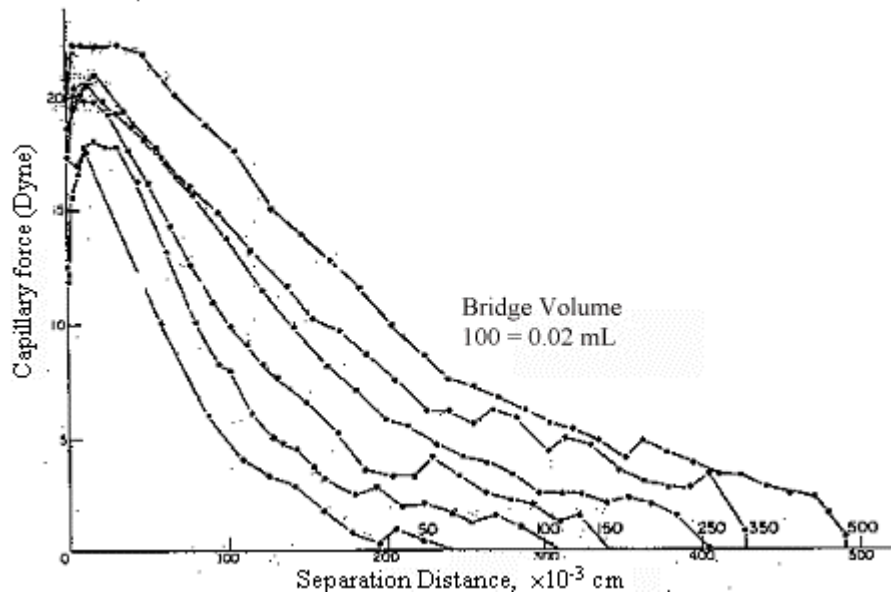


Figure 8. Capillary force variations with particle detachment at constant bridge volume (After Mason and Clark [17])